Decision Fusion for Robust Horizon Estimation using Dempster Shafer Combination Rule

Ramesh Ashok Tabib*
Dept. of CSE,
SDMCET, Dharwad
rameshashoktabib@gmail.com

Ujwala Patil
Dept. of E&C,
BVBCET, Hubli
ujwalapatil@bvb.edu

Syed Altaf Ganihar
Dept. of E&C,
BVBCET, Hubli
altafganihar@gmail.com

Neeta Trivedi
AIEL, ADE,
DRDO, Bangalore
neeta.trivedi@gmail.com

Uma Mudenagudi
Dept. of E&C,
BVBCET, Hubli
uma@bvb.edu

***Abstract*—In this paper, we address the problem of decision fusion for robust horizon estimation using Dempster Shafer Combination Rule (DSCR). We provide a framework for decision fusion to select robust horizon estimate out of 'n' estimates, based on confidence factor. Vision-based attitude estimation depends on robust horizon estimation and no single algorithm gives accurate results for different kind of scenarios. We propose to combine the evidence parameters to generate confidence factor using DSCR to justify the correctness of the estimated horizon. We compute Confidence Interval (CI) based on Gaussian Mixture Model (GMM). We also propose two techniques to provide evidence parameters for the estimated horizon using CI. We demonstrate the effectiveness of the decision framework on clear and noisy data sets of simulated and real images/videos captured by Micro Air Vehicle (MAV).**

I. Introduction

In this paper, we propose a decision framework which combines different methods of horizon estimation (HE) and selects the estimate of horizon with highest confidence factor. We compute confidence factor by combining evidence parameters using Dempster Shafer's Combination Rule (DSCR) [1]. We propose two methods to compute evidence parameters based on Confidence Interval (CI) which is computed using GMM. We demonstrate proposed decision fusion framework on estimates of horizon using two methods. These estimates are used for the attitude estimation of Micro Air Vehicles (MAV) [2].

Many methods have been proposed in the literature for horizon estimation. Authors in [3] [4] address techniques for horizon estimation by segmenting the sky and the non-sky region based on the color. Due to the change in the sky-color, this method is expected to fail [5]. Another class of methods proposed in [6] [7] use detection of edge, however they fail when frames contain stray edges. Author in [8] uses texture to differentiate the ground and the sky region where the disadvantage is, these methods are data dependent and need large training sets and the time complexity is high. The estimates of horizon provided by most of the methods may go erroneous when conditions are non-favourable and there is no indication of the results being erroneous.

In this paper, we address the problem by providing robust estimates of horizon using decision fusion framework. According to our knowledge there is no literature on decision fusion for the estimation of horizon by combining different horizon estimates. We propose a novel framework to combine different horizon estimates to provide the robust horizon estimate.

The main contributions of the paper are:

1) We provide framework for decision fusion to select robust horizon estimate based on confidence factor.
2) We propose to determine Confidence Interval (CI) for the estimated horizon based on GMM.
3) We propose two techniques to provide evidence parameters for the estimated horizon based on CI.
4) We provide a framework for combining evidence parameters to generate confidence factor using DSCR.

We present the proposed framework in Section II, discussion of results in Section III and conclusions in Section IV.

II. Framework for Decision Fusion

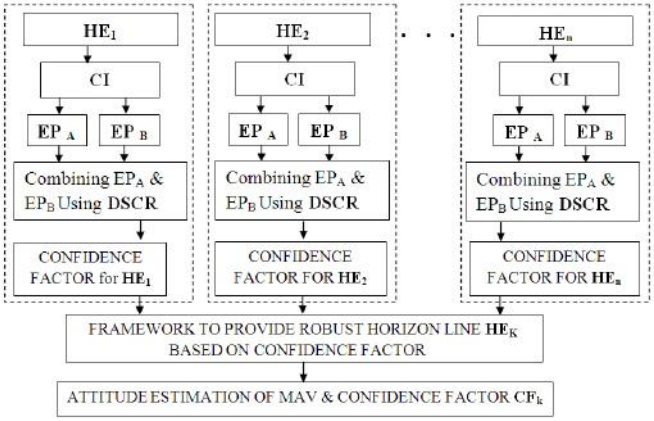

Fig. 1. Decision Fusion Framework

The block diagram of proposed decision fusion framework is shown in Fig 1. The framework combines n different horizon estimates $\{HE_1, \ldots, HE_n\}$ and selects the robust estimate of horizon HE_k with highest confidence factor. We provide a Confidence Interval (CI) around the estimated horizon, that depend on the defined accuracy for the horizon. We compute the CI around the horizon by modeling the non-sky and sky pixels as Gaussian normal distribution and pixels inside the CI as Gaussian Mixture Model (GMM). To estimate the confidence factor of the estimated horizon, we need evidences justifying the correctness of the horizon. As the confidence of the estimated horizon cannot be reliably predicted using evidence provided by only one method, we propose two methods EP_A and EP_B to provide evidence parameters. The method EP_A is based on the voting by the boundary points and the method EP_B is a patch based method, which use the computed CI to estimate the evidence parameter. These

evidence parameters are combined to compute confidence factor using DSCR for each of the estimated horizon which contributes in the decision fusion.

In what follows, we explain computation of confidence interval, evidence parameters and confidence factor.

A. Confidence Interval (CI)

We provide a confidence interval around the estimated horizon, which depend on the defined accuracy level γ [9]. The confidence interval for the non-sky and sky points considered above and below the estimated horizon respectively can be determined by selecting a suitable confidence level γ for the distribution. For a given γ, the value $z = f(\gamma)$ for the CI is computed from the t-distribution table [9] corresponding to the defined accuracy level. We consider γ to be 95% and corresponding value for $z = 1.96$. The CI for the given accuracy level γ [9] is,

$$\widetilde{CONF}_{\gamma}\{m - zSE_j \leq \mu_j \leq m + zSE_j\} \tag{1}$$

where, m is the mean of pixels defining the horizon, μ_j is the mean of the sampling distribution of either sky or non-sky points under consideration and SE is the standard error of the sampling distribution with respect to the mean m, and is, $SE_j = |\Sigma_j|^{\frac{1}{2}}/\sqrt{N}$ where, N is the number of boundary pixels.

We compute the CI around the horizon by modeling the non-sky and sky pixels as Gaussian normal distribution and pixels inside the CI as Gaussian Mixture Model (GMM). Let, x be a pixel inside the CI and is modeled as GMM. The Probability Distribution Function (PDF) of x is computed as the weighted sum of Gaussians for the sky and non-sky distributions and is given by [10],

$$p(x|\theta) = \sum_{j=1}^{C} \pi_j \mathcal{N}(x|\mu_j, \Sigma_j) \tag{2}$$

where, j denotes the index which runs from 1 to C and in our case $C = 2$ (if $j = 1$, then non-sky regions and if $j = 2$, then sky regions), π_j is the weight of the component j, θ is the parameter list for the GMM probability density function and $\mathcal{N}(x|\mu_j, \Sigma_j)$ is the PDF for the individual Gaussian normal distribution [9][11].

The sample means μ_j and the variances Σ_j for the sky and non-sky points can be calculated by the principle of maximum likelihood estimates for the Bayesian Gaussian mixture model. The *aposterior* probability of a mixture component given a data point is given by [10],

$$P(x_j|x, \theta) = \frac{\mathcal{N}(x|x_j, \theta)P(x_j|\theta)}{p(x|\theta)} \tag{3}$$

where, $P(x_j|\theta) = \pi_j$ is the weight of the individual normal distribution and $\mathcal{N}(x|x_j, \theta)$ is the PDF for the individual Gaussian normal distributions. The maximum likelihood estimates [11] gives the sample mean and the variance [10] as,

$$\mu_j = \frac{\sum_{j=1}^{N} P(x_j|x, \theta)x}{\sum_{j=1}^{N} P(x_j|x, \theta)}, \quad \Sigma_j = \frac{\sum_{j=1}^{N} P(x_j|x, \theta)(x - \mu_j)^2}{\sum_{j=1}^{N} P(x_j|x, \theta)} \tag{4}$$

The values for the individual sample means and variances can then be used for the estimation of the confidence intervals for the Bayesian GMM given by,

$$CONF_{\gamma}\{m - zSE_2 \leq \mu_j \leq m + zSE_1\} \tag{5}$$

where, the lower bound is determined by the confidence interval for the sky distribution points below the horizon and the upper bound is determined by the confidence interval for the non-sky distribution points above the horizon (see Fig 2).

B. Evidence Parameters

We propose two methods EP_A and EP_B to provide evidence parameters, which are required to justify the correctness of the estimated horizon. The method EP_A is based on the voting by the boundary points and the method EP_B is patch based method where the region around the estimated horizon is used to generate evidence parameter. The computed Confidence Interval (CI) is used to compute the evidence parameter.

1) Voting based method (EP_A): The points on the boundary of the sky and ground are detected by registering transition in intensities. The voting scheme includes *m-out-of-n* voting in which the m votes agree out of n contributors towards the hypothesis. This is a variant of *m-out-of-n* voting, in which the vote is considered if boundary point v_i lies in the confidence interval stated in equation (5). The evidence parameter towards belief is given by, $EP_{A1} = (\sum_{i=1}^{n} v_i)/n$. v_i can take either '0' or '1'. v_i=1, if it lies in the confidence interval, and v_i=0 if it lies outside (see Fig 2). The evidence of disbelief is given by, $EP_{A2} = 1 - EP_{A1}$. The ambiguity towards the hypothesis is given by, $EP_{A3} = 0$, as there is no ambiguity considered in this method.

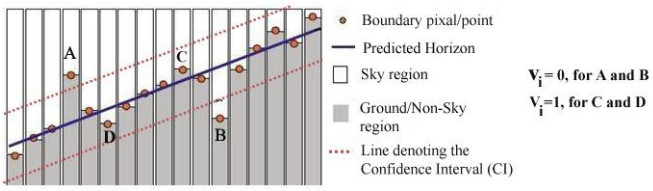

Fig. 2. The CI and the distribution of boundary points.

2) Patch based method (EP_B): The confidence interval (CI) described in Section 2.1 is divided into patches of 5x5 as shown in the Fig 3. If all the pixels inside the patch belongs to sky then the patch is considered as pure sky (X_S) and similarly, if all the pixels inside the patch belongs to non-sky then the patch is considered as pure non-sky (X_N). The patches containing both sky and non-sky pixels are considered as ambiguous (X_A) (see Fig 3). The sky patch above and non-sky patch below the horizon contributes towards the belief EP_{B1} in favor of horizon and is given by, EP_{B1}=$P(X_B) = P(X_S|S)P(S) + P(X_N|N)P(N)$. Similarly, the sky patch below and non-sky above the horizon contributes towards the disbelief EP_{B2} against the horizon and is given by, EP_{B2} =$P(X_D) = P(X_S|N)P(N) + P(X_N|S)P(S)$. The ambiguous patches contribute towards the ambiguity EP_{B3} and is given by, EP_{B3}=$P(X_{Amb}) = P(X_A|N)P(N) + P(X_A|S)P(S)$.

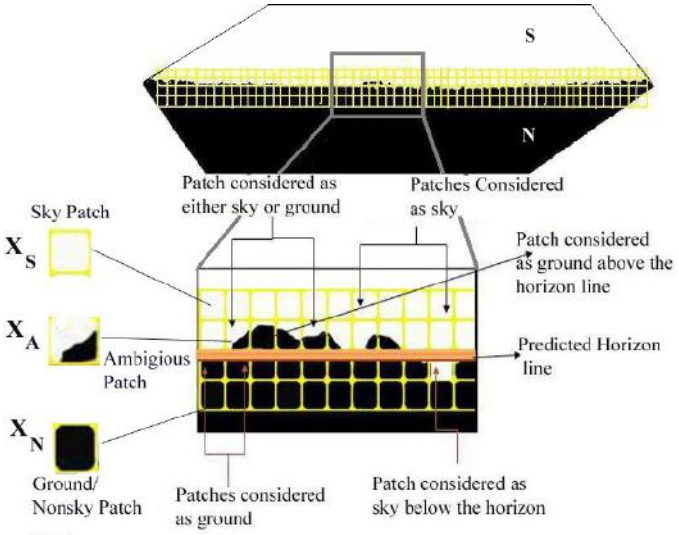

Fig. 3. The Patch distribution in CI

These evidence parameters are considered as the masses for the belief function in Dempster Shafer Combination Rule (DSCR).

C. Confidence Factor

We provide confidence factor for decision fusion using Dempster Shafer Combination Rule (DSCR) to combine the mass of evidences provided by two methods of generating evidence parameter [12] [13] [14]. The decision framework uses confidence factor to select robust horizon out of n different horizon estimates. Let, h_1 and h_2 be the confidence for belief and disbelief towards the estimated horizon respectively. We denote the states of the complete system in a set as, $2^{\Omega} = \{\emptyset, \{h_1\}, \{h_2\}, \Omega\}$ where, $\Omega = \{h_1, h_2\}$ denotes the ambiguity state and $\emptyset$ denotes the conflict between the sets. Dempster Shafer, suggested a rule of combination [12] which combines the evidence as masses EP_A and EP_B. Let, Z be the combined hypothesis, then according to the DSCR, the numerator in equation (6) and (7) represents the accumulated evidence for EP_A and EP_B, which supports the hypothesis Z. Denominator summation in equation (6) quantifies the mass of conflict about the hypothesis. The denominator in equation (7) (*viz.* $(1 - \emptyset)$), specifies about the total mass due to belief, disbelief and ambiguity towards the hypothesis, which acts as the normalization factor towards the hypothesis.

The mass of combined hypothesis Z is given by,

$$m(Z) = \frac{\sum_{EP_A \cap EP_B = Z \neq \phi} m(EP_A).m(EP_B)}{1 - \sum_{EP_A \cap EP_B = \phi} m(EP_A).m(EP_B)} \quad (6)$$

which can be written as,

$$m(Z) = \frac{\sum_{EP_A \cap EP_B = Z \neq \phi} m(EP_A).m(EP_B)}{\sum_{EP_A \cap EP_B \neq \phi} m(EP_A).m(EP_B)} \quad (7)$$

The subset contributing towards belief of hypothesis is, $\{h_1\} = \{m(Z_{11}), m(Z_{13}), m(Z_{31})\} = \{m(K_1), m(K_2), m(K_3)\}$. Similarly, the subset contributing towards disbelief is, $\{h_2\} = \{m(Z_{22}), m(Z_{23}), m(Z_{32})\} = \{m(K_4), m(K_5), m(K_6)\}$. The subset contributing towards both belief and disbelief is null set, $\{\emptyset\} = \{m(Z_{12}), m(Z_{21})\}$. The set which is ambiguous is, $\{\Omega\} = \{m(Z_{33})\} = \{m(K_7)\}$. The mass of the hypothesis $\{h_1\}$ and $\{h_2\}$ as per the equation (7) are given by,

$$m(\{h_1\}) = \frac{\sum_{i=1}^{3} m(K_i)}{\sum_{i=1}^{7} m(K_i)}, \quad m(\{h_2\}) = \frac{\sum_{i=4}^{6} m(K_i)}{\sum_{i=1}^{7} m(K_i)} \quad (8)$$

The masses $m(\{h_1\})$ and $m(\{h_2\})$ are the values of confidence factor in favour (CF_1) and against (CF_0) the estimated horizon respectively. The confidence factor CF_1 provides the accuracy of estimated horizon. We use two methods Hough [15] and RANSAC [16] to estimate the horizon. We compute CF_1 for Hough transform and RANSAC as (CF_1^h) and (CF_1^r) respectively and select robust horizon estimate HE_k with highest confidence factor (CF_K).

TABLE I. THE COMBINATION TABLE CONTAINS THE FULL PLOT OF COMBINED HYPOTHESES OF EP_A AND EP_B [12].

$\cap$	$m(EP_{B1})$	$m(EP_{B2})$	$m(EP_{B3})$
$m(EP_{A1})$	$h_1 \leftarrow m(Z_{11})$	$\emptyset$	$h_1 \leftarrow m(Z_{13})$
$m(EP_{A2})$	$\emptyset$	$h_2 \leftarrow m(Z_{22})$	$h_2 \leftarrow m(Z_{23})$
$m(EP_{A3})$	$h_1 \leftarrow m(Z_{31})$	$h_2 \leftarrow m(Z_{32})$	$\Omega \leftarrow m(Z_{33})$

III. RESULTS AND DISCUSSION

We demonstrate the effectiveness of the proposed framework for decision fusion using real videos of clear and noisy data set. We test proposed framework on four input videos with 100 frames in each input video where two videos are clear and two are noisy. We run our algorithm on Intel(R) Core(TM)2 Duo T5250 processor with 1GB RAM.

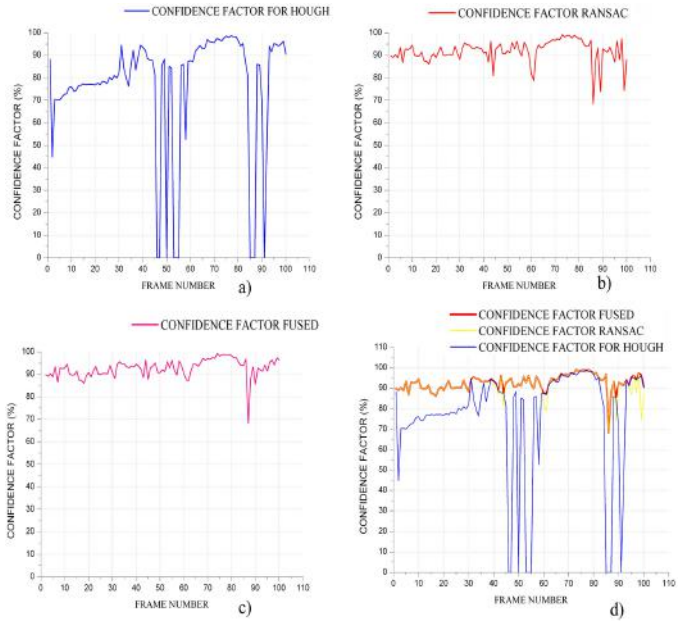

Fig. 4. Graphs Showing the Confidence Factor (CF) for 100 frames of Clear video (a) CF using Hough (b) CF using RANSAC (c) CF after Fusion (d) All a, b, c plots combined.

Fig 4 illustrates the plot of the confidence factor for 100 frames of the video of clear image dataset using Hough and RANSAC method of horizon estimation. Fig 4(a) and Fig 4(b) illustrates the plot of the confidence factor using Hough and RANSAC respectively. Fig 4(c) and Fig 4(d) illustrates the plot

of the confidence factor after fusion. In Fig 4(c) and Fig 4(d) we can see that confidence factor of fused is better than the individual confidence factors of Hough and RANSAC shown in Fig 4(a) and Fig 4(b).

The Fig 5(a)-(l) demonstrate the output of fusion framework. The column-1 and column-2 of Fig 5 represent results of Hough and RANSAC method respectively and the final fused output provides the horizon with highest confidence factor, which is shown in column-3. If $CF_1^h > CF_1^r$, we denote the horizon in yellow, and red if visa-versa. Row-1 of Fig 5 demonstrates case where, both CF_1^r and CF_1^h are high. Similarly, Row-2 where, $CF_1^h > CF_1^r$, Row-3 where, $CF_1^h < CF_1^r$ and Row-4 where, both CF_1^r and CF_1^h are low.

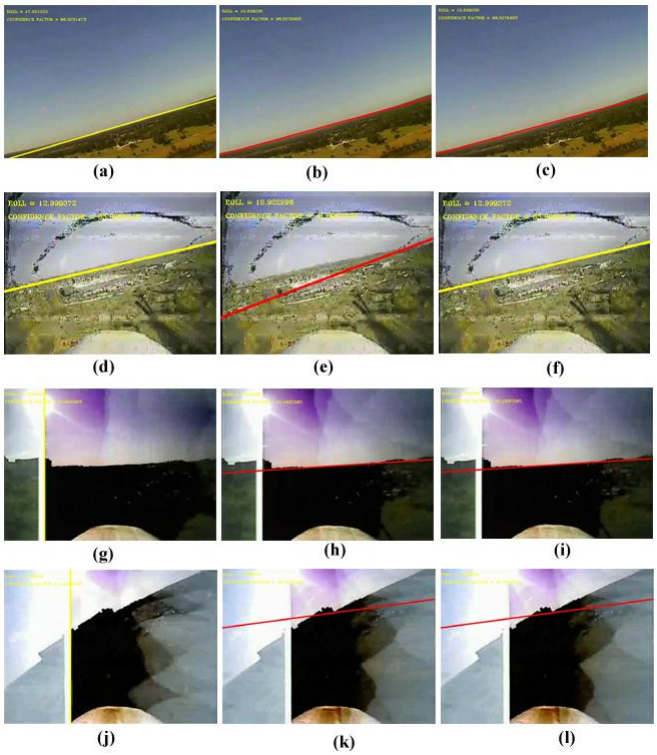

Confidence factor of image: a) 98.32%, b) 98.55%, c) 98.55%, d) 83.9%, e) 71.07%, f) 83.9%, g) 0%, h) 85.29%, i) 85.29%, j) 0%, k) 35.78% , l)35.78%

Fig. 5. Results of Decision framework: (a, d, g, j) For Hough, (b, e, h, k) For RANSAC, (c, f, i, l) Robust horizon estimates after fusion.

TABLE II. AVERAGE CONFIDENCE FACTOR FOR THE DATA SET.

Data sets		Average CF_r in %	Average CF_h in %	Average CF_k in %
Clear	$Video-1$	91.79 %	76.31%	92.65%
	$Video-2$	87.22%	94.08%	95.84%
Noisy	$Video-3$	70.6%	30.73%	71.72%
	$Video-4$	68.49%	44.89%	71.89%

Table II shows the average confidence factor for the data set. We can see that the average confidence factor CF_k *i.e* the confidence factor after fusion is better than the individual confidence factors CF_h and CF_r for all four videos.

IV. CONCLUSION

We have addressed the problem of decision fusion for robust horizon estimation. We have provided framework for decision fusion to select robust horizon estimate based on confidence factor using Dempster Shafers Combination Rule (DSCR). We propose to determine Confidence Interval (CI) for the estimated horizon based on GMM. We have provided two techniques to compute evidence parameters for the estimated horizon based on CI by voting of boundary points and by patch based method. The confidence factor is estimated by combining two evidence parameters using DSCR. We have demonstrated the framework using Hough transform and RANSAC based horizon estimation on clear and noisy videos from Micro air vehicle (MAV). The framework can be extended to fuse 'n' number of horizon estimates. The estimate of horizon having highest confidence factor is used for attitude estimation of MAV.

REFERENCES

[1] U. G. Mangai, S. Samanta, S. Das, and P. R. Chowdhury, "A survey of decision fusion and feature fusion strategies for pattern classification," *IETE*, vol. 27, pp. 293–307, July-August 2010.

[2] S. Thurrowgood, R. J. D. Moore, D. Bland, D. Soccol, and M. V. Srinivasan, "Uav attitude control using the visual horizon," *Australasian Conference on Robotics and Automation (ACRA 2010)*, pp. 1–3, December 2010.

[3] J. Luo and S. Etz, "A physics-motivated approach to detecting sky in photographs," *Proceedings of the 16th International Conference on Pattern Recognition*, pp. 155–158, August 2002.

[4] H. Chao, "Autopilots for small fixed-wing unmanned air vehicles: A survey," *International Conference on Mechatronics and Automation, ICMA 2007*, pp. 3144–3149.

[5] H.-Z. Yuan, X.-Q. Zhang, and Z.-L. Feng, "Horizon detection in foggy aerial image," *International Conference on Image Analysis and Signal Processing (IASP)*, pp. 191–194, April 2010.

[6] M. Hwangbo, "Robust monocular vision-based navigation for a miniature fixed-wing aircraft," *PhD Thesis, Robotics Institute Carnegie Mellon University Pittsburgh, Pennsylvania*, September 2009.

[7] Zafarifar, Bahman, Weda, Hans, de with, and P. H. N, "Horizon detection based on sky-color and edge features," vol. 6822, pp. 682220–682229, Visual Communications and Image Processing, 2008.

[8] S. Fefilatyev, V. Smarodzinava, L. O. Hall, and D. B. Goldgof, "Horizon detection using machine learning techniques," in *5th International Conference on Machine Learning and Applications, 2006. ICMLA '06*, pp. 17–21, dec. 2006.

[9] J. L. Devore, *Probability and statistics for engineering and sciences*. Boston, USA: Brooks/Cole Cengage learning, 8 ed., 2012.

[10] A. Dempster, L. N, and R. D, "Maximum likelihood from incomplete data via the em algorithm," *Journal of Royal Statistical Society*, vol. 39, pp. 1–38, 1977.

[11] R. Duda, P. Hart, and D. Stork, *Pattern Classification*. John Wiley and Sons, 2 ed., 2001.

[12] R. U. Kay, "Fundamentals of the dempster-shafer theory and its applications to system safety and reliability modeling," *RTA Special Issue*, pp. 3–4, December 2007.

[13] Dempster and A. P. Shafer, "A generalization of bayesian inference," *Journal of the Royal Statistical Society*, vol. 30, pp. 205–247, 1968.

[14] C. Thomas and N. Balakrishnan, "Modified evidence theory for performance enhancement of intrusion detection systems," *11th International Conference on Information Fusion*, pp. 1–8, July 2008.

[15] R. C. Gonzalez and R. E. Woods, *Digital image processing*. Upper Saddle River, N.J.: Prentice Hall, 2 ed., 2002.

[16] M. A. Fischler and R. C. Bolles, "Random sample consensus: A paradigm for model fitting with applications to image analysis and automated cartography," *Comm. of the ACM*, vol. 24, pp. 381–395, June 1981.